

Electrorheological fluid-actuated microfluidic pump

Liyu Liu, Xiaoqing Chen, Xize Niu, Weijia Wen,^{a)} and Ping Sheng
Institute of Nano Science and Technology, Department of Physics, The Hong Kong University of Science and Technology, Clear Water Bay, Kowloon, Hong Kong, China

(Received 22 May 2006; accepted 29 June 2006; published online 22 August 2006)

The authors report the design and implementation of an electrorheological (ER) fluid-actuated microfluidic pump, with programmable digital control. Our microfluidic pump has a multilayered structure fabricated on polydimethylsiloxane by soft-lithographic technique. The ER microfluidic pump exhibits good performance at high pumping frequencies and uniform liquid flow characteristics. It can be easily integrated with other microfluidic components. The programmable control also gives the device flexibility in its operations. © 2006 American Institute of Physics. [DOI: 10.1063/1.2337877]

Microfluidic chips have been widely studied and designed to realize functions such as the cell lysis, purifications¹ and analysis in bioapplications,² sensors for the liquid fronts,³ droplet controls⁴ and even optical applications,⁵ etc. To drive the fluid inside the chips, micropump is a necessary component of all the microfluidic chips, regardless of the applications. Various types of pumps have been designed and fabricated using different mechanisms, e.g., gas pump is actuated and controlled by gas^{6,7} and piezoelectric transducer actuator pump utilizes electrical/mechanical energy conversion.⁸ There is also the electro-osmosis pump⁹ for pumping ionic solutions, e.g., NaCl and KCl. Here we present an application of the electrorheological (ER) fluid in the design and fabrication of a micropump, with programmable digital control.

ER fluid is a type of colloidal suspension whose rheological characteristics can be controlled through the application of an external electric field. With the discovery of the giant electro-rheological (GER) effect,¹⁰ GER fluid can have high shear stress and fast response time (within 10 ms), making it an ideal material for microfluidic applications.¹¹ The present micropump is fabricated on polydimethylsiloxane (PDMS), offering ease of fabrication and biocompatibility.

Figure 1 shows the schematic diagram of a five-layer structure inside the PDMS chip, 36 mm in length and 25 mm in width. ER fluid channels, located in the bottom layer, are divided into three parallel branches. These 500 μm wide channels, sandwiched by a pair of electrodes (carbon black and PDMS composite), have two conjunct inlet and outlet tubes through which ER fluid is circulated. All electrodes are labeled from A to H as shown in the figure. For simplicity, the middle channels are designed to share common electrodes with the channels to the right and left, e.g., the middle channel share electrodes B and F with the channels to the right and electrodes C and G share with the channels to the left, respectively. Three circular diaphragms, 1 mm in radius and 30 μm thick, are located between the two pairs of electrodes of every channel as indicated in Fig. 1. Another square fluid channel (0.6 mm wide and 1 mm deep) on the top layer is used for (pumped) circulating fluid, wherein a 1.8 mm wide cell is set right over the three diaphragms. The cell has an arc-roof structure which is 200 μm high at the edge and

400 μm high in the middle. Within this zone, the ER fluid underneath can affect the flow of the pumped fluid via the pull-push movement of the diaphragms. The cooperative movements of the diaphragms actuated by the ER fluid valves are the direct driving mechanism for pumping, i.e., the clockwise flow indicated in the figure is realized by adjusting the alternate, cooperative movement of the three diaphragms. The right upper inset of Fig. 1 is the top view of the fabricated micropumping system.

Figure 2(a) is a top view showing the control principle of the ER valves, where the flows of ER fluid within the channels can be controlled when an external electric field is applied to the electrodes. That is, when the voltage on one pair of electrodes is applied, the viscosity of the ER fluid increases between the electrodes, thereby lowering the flow velocity of ER fluid. The flow can even be stopped if the voltage is high enough. The top left panel in Fig. 2(a) shows the situation in which the ER fluid flows from right to left when an adequate voltage is applied only on the left pair of electrodes. In this case, the ER flow is stopped to the left, thus causing the pressure to accumulate under the diaphragm and pushing it upward, as shown in red. The (pumped) fluid volume over the diaphragm is compressed and the fluid in the area is repelled. The top right panel shows the situation

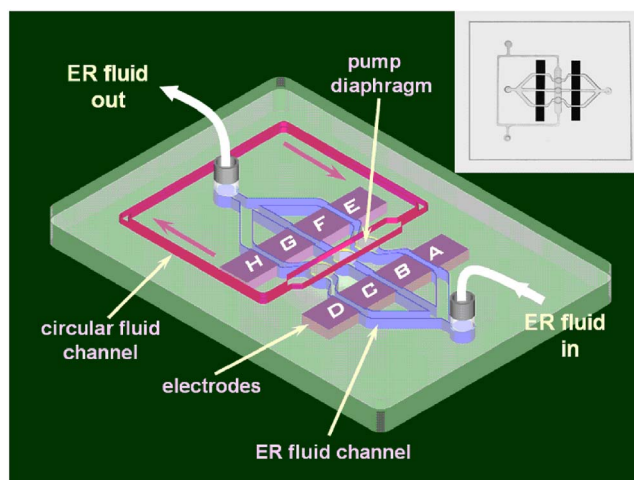


FIG. 1. (Color online) Schematic illustration of the micropump, with its three-dimensional structure, inside the microfluidic chip. The chip actuated by ER fluid controls the fluid circulation in the upper layer. The right upper inset is a picture of the fabricated device.

^{a)}Electronic mail: phwen@ust.hk

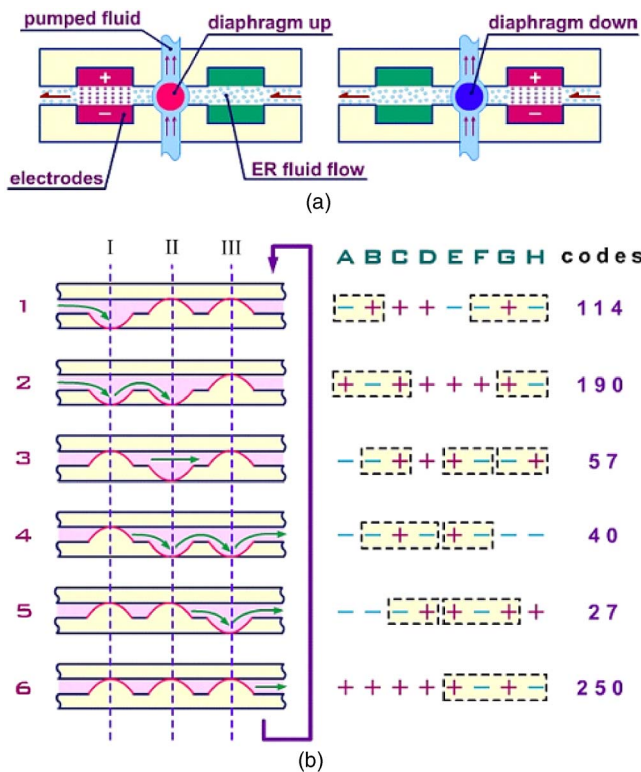


FIG. 2. (Color online) In (a) the principle of ER valve’s operation is illustrated schematically by showing the deformation of a single diaphragm via pumped ER fluid. The diaphragms’ pumping sequences and their corresponding signals are shown in (b).

when the ER fluid is stopped by the right pair of electrodes, thus causing the pressure to decrease within the channel and thereby pulling the diaphragm downward. The (pumped) fluid volume over it then expands and imbibes more fluid into the local region. These repelling and imbibing actions, when controlled via electrical signals to act cooperatively, can give rise to the desired pumping action.

Figure 2(b) illustrates the principle of the micropump and the corresponding control modes. The left panel is a cutaway view of the flows, where all steps are listed and labeled¹² from 1 to 6. To control the system accurately, only one diaphragm is set to take action in each time step. Dashed lines are employed to show the locations of the diaphragms, and the arrows indicate the primary streaming direction(s) of the pumped fluid. The pumping action results from the diaphragms following the sequential steps 1–6, followed by the iteration of the whole sequence. To realize each action step, voltages are applied on the labeled electrodes with positive and negative potentials as shown in the right panel. For instance, in step 1 when “AB,” “FG” and “GH” are charged,

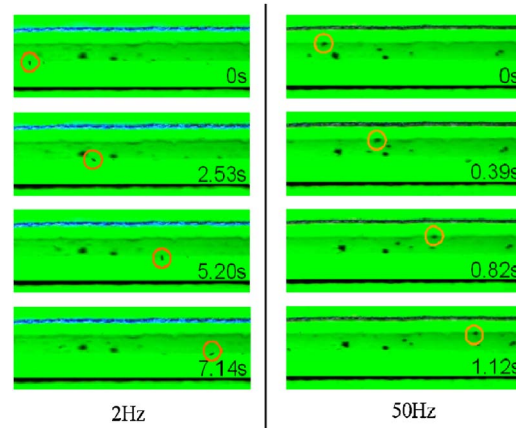


FIG. 3. (Color online) Circles indicate the locations of a particle at specific times. The flow rates with signal frequencies of 2 and 50 Hz are shown in the left and right panels, respectively. Some black particles at rest are those which have subsided and stuck to the channel wall. These can be ignored.

the corresponding valves are closed, making the diaphragm “I” to move downward and diaphragms “II” and “III” to bulge up. As there are eight electrodes which can be independently controlled, we are able to digitize the signals so that the voltages are expressed and managed with binary codes, listed on the right panel. Besides the tunable voltages, digitized programmable control offers flexibility (e.g., reversing the pumping flow direction) and adjustable individual action steps.

In order to visually capture the pumped flow, we use polystyrene particles of 250 μm in diameter dispersed in oil. A charge-coupled device camera is employed to record the pumping action. Figure 3 shows the motions of styrene particles through the pumping channel. In the images, circles are used to trace the locations of a particle observed at different instants of time. The left four panels show the fluid motions when the electrical signals are applied at the frequency of 2 Hz, i.e., the diaphragms take one single action in 0.5 s, while the right panels show the case at 50 Hz. Compared with the 2 Hz case, the higher frequency of applied electrical signals gives rise to faster flows, although the relationship is not linear. It is also observed that although the flow moves forward as a whole, at some signal steps, such as 1, 2, and 4, there can be some backward flow. This is because in these steps, diaphragms concave downward so that certain volume of fluid ahead can be sucked backward. This effect is more apparent at low frequencies than at higher frequencies.

Pumped flux is a measure of the effectiveness of a micropump. As the flow is Poiseuille in character, we measure the particles at the $\sim 1/4$ or $\sim 3/4$ width points across the

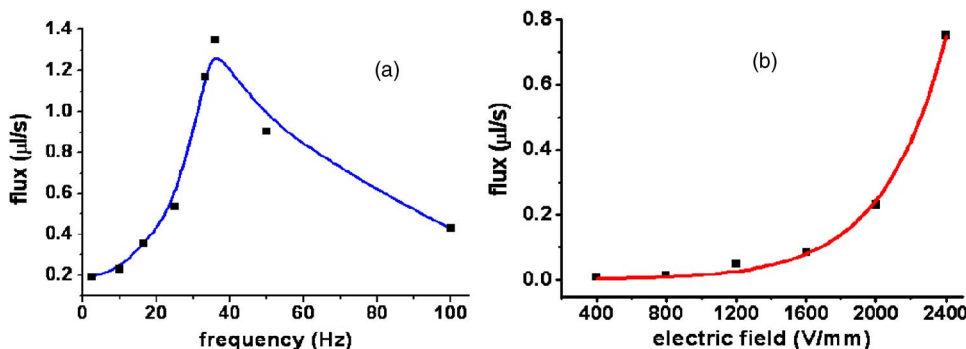


FIG. 4. (Color online) Flux of the pumped fluid plotted as a function of the signal frequency or the applied electric field across the channels, shown, respectively, in the left and right panels.

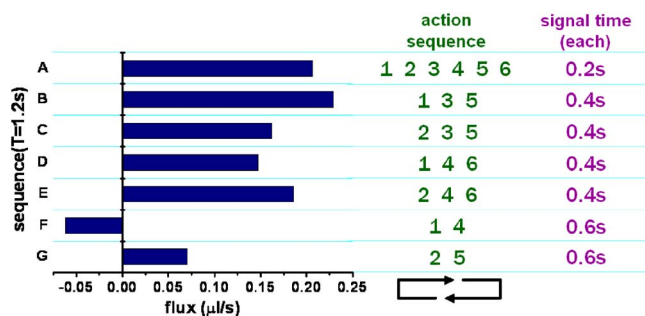


FIG. 5. (Color online) Functions on the flux with simplified pumping sequences programmed and controlled by the digital signals. The left is the series of flux described in histograms with the corresponding detailed sequences and signal time on the right.

channel. These particles should have the speed $\sim(1/2)V_{\max}$ of the parabolic flow profile. The flow rate is in turn measured by recording the particle locations (along the flow direction) at various instants of time. Thus the pumped flux can be obtained by multiplying the measured average speed with the cross sectional area. In Fig. 4, the pumped flux measured in this manner is plotted as a function of signal frequency (A) and the electric field (B). Figure 4(a) shows the pumped flux reaching a peak at ~ 35 Hz when all the electric signals have the strength of 2 kV/mm. The peak is the result of the competition between higher pumping frequency and the response time required for the pumped fluid in each action step of the sequence. At high frequencies, pressure cannot reach the desired value in ER fluid valves during the single action period, so the diaphragms would not be able to attain the required deformations to either repel or imbibe the proper amount of pumped fluid. Thus the pumping effectiveness suffers.

Variation of the pumped flux with the applied electric field is shown in Fig. 4(b). The frequency is fixed at 10 Hz. The result shows that the flux increases monotonically with the field. The data can be well fitted by an exponential dependence, shown as the red line.

The direction of fluid flow and the pumped flux can also be controlled through digitized programmable sequences. As the original pumping procedure takes a total of six action steps per sequence, some simplification and optimization can be envisaged. Figure 5 lists the attained flux under different action sequences, labeled from A to G. For each sequence, the corresponding action steps are enumerated on the right side, with each number corresponding to the action shown in Fig 2(b). All sequences are set to be 1.2 s in duration,

equally shared by the action steps within a single sequence. For example, sequence C has action steps 2, 3, and 5; hence 0.4 s is allocated to each step. All sequences are iterated. The results reveal that the flux can vary with the programmed sequence. For example, sequence B with simplified three-action step iteration can attain a higher pumped flux to the original six-action step sequence (A). In this sequence, the pumped fluid seems to form packets, passing over the diaphragms in a wormlike motion. Also, a more smooth flow has been observed at this low frequency. Sequences F and G have the fewest action steps. In the first action step, the two adjacent diaphragms deform synchronously and the other one 180° out of phase, and the second step is the reverse of the first action step. The pumped fluxes in sequences F and G have almost the same value but opposite flow directions. These results show that programmed sequence can be an important factor in affecting the pumping efficiency.

Owing to its simple design, flexibility, ease in control, and material biocompatibility for integration with other microfluidic components, this ER-fluid based micropump is seen to have wide potential applications, such as transporting and generating uniform microfluid in inspection systems, constructing circular flow paths for rinsing cells in a biochip, cooling components in microdevice, etc.

The authors wish to acknowledge the support of Hong Kong RGC Grant No. 604104.

- ¹J. W. Hong, V. Studer, G. Hang, W. F. Anderson, and S. R. Quake, *Nat. Biotechnol.* **22**, 435 (2004).
- ²P. Sabouchi, C. I. Zanetti, R. Chen, M. Karandikar, J. Seo, and L. P. Lee, *Appl. Phys. Lett.* **88**, 183901 (2006).
- ³K. S. Ryu, K. Shaikh, E. Goluch, and C. Liu, *Appl. Phys. Lett.* **88**, 104104 (2006).
- ⁴K. Ahn, C. Kerbage, T. P. Hunt, R. M. Westervelt, D. R. Link, and D. A. Weitz, *Appl. Phys. Lett.* **88**, 024104 (2006).
- ⁵U. Levy, K. Campbell, A. Groisman, S. Mookherjea, and Y. Fainman, *Appl. Phys. Lett.* **88**, 111107 (2006).
- ⁶C. F. Lin, G. B. Lee, C. H. Wang, H. H. Lee, W. Y. Liao, and T. C. Chou, *Biosens. Bioelectron.* **21**, 1468 (2006).
- ⁷M. A. Unger, H. P. Chou, T. Thorsen, A. Scherer, and S. R. Quake, *Science* **288**, 113 (2000).
- ⁸N. T. Nguyen and T. Q. Truong, *Sens. Actuators B* **97**, 137 (2004).
- ⁹T. Hasegawa, S. Toga, M. Morita, T. Narumi, and N. Uesaka, *JSME Int. J., Ser. B* **47**, 557 (2004).
- ¹⁰W. Wen, X. Huang, S. Yang, K. Lu, and P. Sheng, *Nat. Mater.* **2**, 727 (2003).
- ¹¹L. Liu, X. Niu, W. Wen, and P. Sheng, *Appl. Phys. Lett.* **88**, 173505 (2006).
- ¹²B. Husband, M. Bu, A. G. R. Evans, and T. Melvin, *J. Micromech. Microeng.* **14**, 64 (2004).